

# Probing the Structure and Energetics of Dislocation Cores in SiGe Alloys through Monte Carlo Simulations\*

Ioannis N. Remediakis,<sup>1,†</sup> David E. Jesson,<sup>2</sup> and Pantelis C. Kelires<sup>1</sup>

<sup>1</sup>*Department of Physics, University of Crete, P.O. Box 2208, 71003 Heraklion, Crete, Greece*

<sup>2</sup>*School of Physics, Monash University, Victoria 3800, Australia*

(Dated: February 6, 2008)

We present a methodology for the investigation of dislocation energetics in segregated alloys based on Monte Carlo simulations which equilibrate the topology and composition of the dislocation core and its surroundings. An environment-dependent partitioning of the system total energy into atomic contributions allows us to link the atomistic picture to continuum elasticity theory. The method is applied to extract core energies and radii of  $60^\circ$  glide dislocations in segregated SiGe alloys which are inaccessible by other methods.

PACS numbers: 61.72.Lk, 61.66.Dk, 61.72.Bb

Dislocations are the most common extended defects in crystalline solids. A prototypical example in semiconductor physics is offered by the generation of dislocations in SiGe alloys grown on Si which relieve the stress induced by the 4% lattice mismatch between Si and Ge [1]. The presence of dislocations in SiGe alloys has a strong impact on their mechanical and electronic properties. Far from the dislocation, the induced strain field depends only on macroscopic properties of the material, such as its shear modulus. However, near the dislocation line, the local properties of the material deviate significantly both from those of the ideal solid and the predictions of continuum elasticity theory. This “core region” of the dislocation, accessible only to atomistic calculations, can have different structures depending on the material, the applied external strain, and other parameters [2].

Although the core structures and energetics of dislocations in elemental crystals have been well studied [3, 4], relatively few investigations have linked the atomistic picture of dislocated alloy systems to traditional continuum descriptions. Blumenau *et al.* used an atomistic description to calculate core structures and energies in perfectly ordered alloys, such as SiC [5]. Martinelli *et al.* performed simulations on SiGe alloys and found that Si-rich and Ge-rich nanowires are formed near the dislocation core [6]. However, despite these important contributions, a well-defined method for extracting core energies and radii from dislocations in segregated alloys has not yet been proposed. In addition, the importance of alloy segregation and its relationship to traditional continuum descriptions including the concept of core parameters is not fully understood.

In view of the crucial role played by dislocations in many important applications for SiGe materials, such as bulk alloy layers for quantum wells [7] or nanoislands for quantum dots [8, 9], it is highly desirable to under-

stand the core energetics and related properties. In the present work, we develop a framework to calculate the core energies and core radii of segregated alloys using atomistic calculations, taking a  $60^\circ$  glide dislocation in a  $\text{Si}_{0.5}\text{Ge}_{0.5}$  alloy as a prototype. This is made possible by an environment-dependent partitioning of the total energy into atomic contributions, which allows us to locally probe the energy at the dislocation core, and link the atomistic picture to continuum theories.

Our approach is based on state-of-the-art continuous-space Monte Carlo (MC) simulations, employing the multi-component empirical potentials of Tersoff [10]. This method, capable of calculating the free energy of the system with great statistical precision, has been applied with success in similar contexts [11, 12]. Three types of random moves are involved in the MC algorithm: atomic displacements, volume changes, and mutual identity exchanges between atoms of different kinds, leading to topological and compositional equilibration of the system, as described in Ref. [12]. The simulation supercell consists of  $40 \times 10 \times 8$  6-atom unit cells of the diamond lattice, with lattice vectors having  $[0\bar{1}1]$ ,  $[1\bar{1}0]$  and  $[111]$  directions, including a total of 19200 atoms. We checked the convergence of our results with respect to the size of the simulation cell by running test simulations with different cell sizes. Epitaxial SiGe alloys grown on Si(100) are simulated by constraining them to have the lattice constant of Si in the supercell, and then allowing relaxation of the lattice vectors only in the  $[100]$  direction.

The most commonly observed dislocations in the diamond lattice are those corresponding to the  $\{111\}$  slip system; the lowest energy perfect dislocation in tetrahedral semiconductors is the so-called  $60^\circ$  glide dislocation [5]. Although such dislocations usually dissociate to Shockley partials, especially in diamond, epitaxially grown alloys are very likely to hold undissociated  $60^\circ$  glide dislocations, due to the strain introduced by the lattice mismatch [13]. We therefore choose to study  $60^\circ$  glide dislocations as characteristic prototypes of dislocations in SiGe alloys. Two such dislocations with opposite

---

\*Accepted for publication in Physical Review Letters.

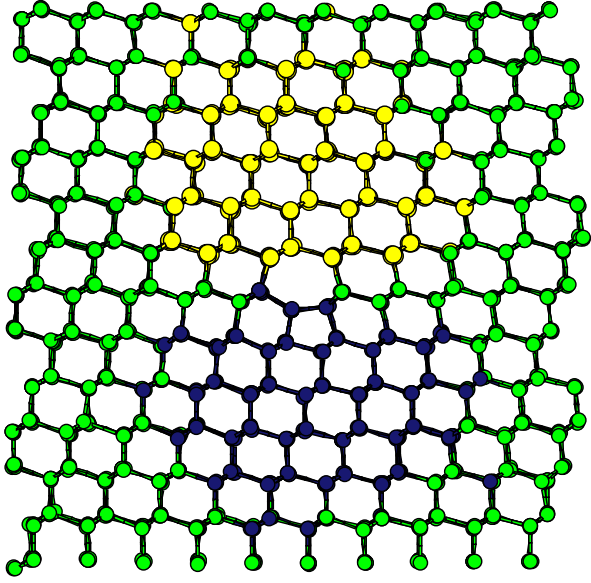


FIG. 1: (color online) Equilibrated structure, 2 nm around the core of a  $60^\circ$  glide dislocation in a  $\text{Si}_{0.5}\text{Ge}_{0.5}$  alloy at 300 K. The dislocation line is normal to the plane of the plot. Sites with  $c \leq 0.3$ , having strong preference for Si, are shown in darkest color; sites with  $c \geq 0.7$ , having strong preference for Ge, are shown in lightest color.

Burgers vectors are introduced in the cell [14], so that the total displacement field away from the dislocation cores is zero. The distance between the dislocation cores is about  $80 \text{ \AA}$ , ensuring that dislocation motion due to mutual interaction can be neglected for the temperatures of our simulations. The Burgers vectors and the lines of the two dislocations lie in the  $[0\bar{1}1]$  and  $[1\bar{1}0]$  direction, respectively.

We begin by equilibrating the unit cell for dislocated bulk SiGe at 300 K. Simulations at higher temperatures (900 K) show similar composition profiles. After several equilibration steps, including identity exchanges, a long run ( $\sim 10^{10}$  MC steps) follows, over which the average occupancy of each site,  $c$ , is calculated. This is defined as the fraction of the simulation time (MC steps) when a site is occupied by a Ge atom over the whole run. Its values range between 0 (site always occupied by Si atoms) and 1 (site always occupied by Ge atoms). For the bulk  $\text{Si}_{0.5}\text{Ge}_{0.5}$  alloy at 300 K, the calculated values of  $c$  are  $0.5 \pm 0.02$ . However, for the cell containing a dislocation, there are sites near the dislocation core with values of  $c$  very close to 0.0 and 1.0, showing strong preference for occupancy by Si or Ge atoms, respectively. This is illustrated in Fig. 1, which shows the equilibrated atomistic structure of the dislocation core. It can be observed that the alloy segregates into Si-rich and Ge-rich cylindrical regions on opposite sides of the dislocation line, which can be viewed as self-assembled nanowires in the alloy

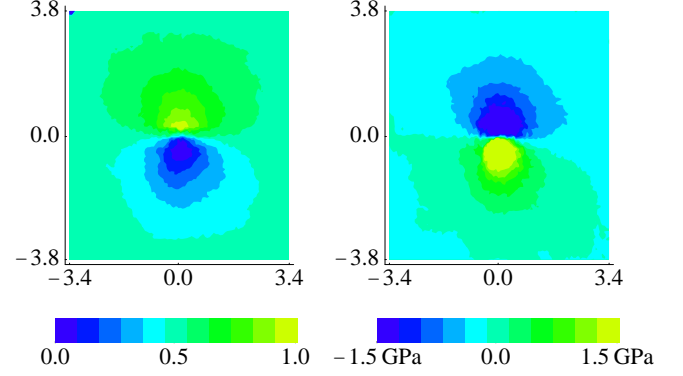


FIG. 2: (color online) Contour plots of the average composition (left) and average atomic stresses (right) around a  $60^\circ$  glide dislocation in a  $\text{Si}_{0.5}\text{Ge}_{0.5}$  alloy at 300 K. The dislocation line is normal to the plane of the plot. Distances shown on the axes of the plots are given in nm.

[6].

To explain this effect we note the similarity to stress induced segregation at the (100) reconstructed surface [11]. The significant near-surface stress field, resulting from surface dimerization, drives smaller atomic volume Si atoms to occupy sites under compression, while the Ge atoms prefer sites under tension. In the present case, this correlation between local stress and composition can be probed via the atomic stress, defined as  $\sigma_i = -dE_i/dV_i$ , where  $E_i$  is the energy of atom  $i$  and  $V_i$  is the volume available to atom  $i$  [11]. In order to link the atomistic picture with macroscopic theories of elasticity, we define a continuous stress field  $\sigma(\mathbf{r}) = \sum_i \sigma_i$ . The sum runs over all atoms  $i$  that have Cartesian positions  $\mathbf{r}_i$  such that  $|\mathbf{r}_i - \mathbf{r}| < 3.0 \text{ \AA}$ . In the same manner, we define a continuous composition field. Fig. 2 shows contour plots of the composition and stress fields on a plane perpendicular to the dislocation line. There is a clear correlation between the two, as Ge atoms prefer to occupy sites under tension while Si atoms prefer sites under compression. The observed composition contours are very similar to those found by lattice Monte Carlo simulations of dislocations in alloys [15].  $\sigma(\mathbf{r})$  has the same qualitative features as the hydrostatic component of the stress tensor around a dislocation,  $\sigma(x, y) \equiv (\sigma_{xx} + \sigma_{yy} + \sigma_{zz})/3 \sim -\frac{y}{x^2 + y^2}$ , as calculated in linear elasticity theory [2]. Similar segregation results are found for both relaxed and epitaxial (100)-constrained alloys.

The significant segregation evident in Fig. 1 will clearly influence the dislocation core energy and elastic properties. It is therefore important to develop a framework for defining dislocation core parameters in the presence of segregation. Our approach is based on a partitioning of the dislocation formation energy into ‘elastic’ and ‘segregation’ components. Consider first the radial dislocation

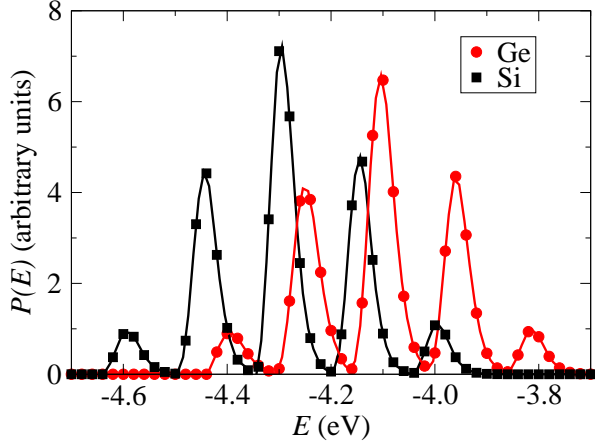


FIG. 3: (color online) Probability density of atomic energies for Si (squares) and Ge (circles) in a  $\text{Si}_{0.5}\text{Ge}_{0.5}$  alloy at 300 K.

formation energy,

$$E_f(R) = \frac{1}{L} \sum_i (E_i - E_{bulk}) \quad (1)$$

where the summation is taken over all atoms  $i$  contained in a cylinder of radius  $R$  and length  $L$  around the dislocation line.  $E_{bulk}$  is the average atomic energy in the random alloy and  $E_i$  is the energy of atom  $i$ . We now decompose the formation energy into two terms,  $E_f(R) = E_{el}(R) + E_{seg}(R)$ , where the elastic and the segregation components are defined as

$$E_{el}(R) = \frac{1}{L} \sum_i (E_i - E(c_i, c'_i)), \quad (2)$$

$$E_{seg}(R) = \frac{1}{L} \sum_i (E(c_i, c'_i) - E_{bulk}). \quad (3)$$

Here, we define  $E(c_i, c'_i)$  as the energy of a site with average occupancy  $c_i$  while the average occupancy of the neighboring sites is  $c'_i$ .  $E_{el}(R)$  represents the energy cost of including a dislocation in a segregated alloy (i.e. an alloy with a compositional fingerprint which is identical to that produced by a dislocation).  $E_{seg}(R)$  is the energy of segregation per unit length of dislocation (i.e. the energy cost of creating the compositional fingerprint from a random alloy). For elemental solids or ordered heteropolar alloys, this is either zero or assumes one of two distinct values and can thus be taken into account implicitly [5]. For a segregated alloy, however, this decomposition is a necessary step in linking atomistic and continuum concepts.

To calculate the elastic and segregation energies defined by Eqs. (2) and (3), we first evaluate the function  $E(c, c')$ . This is achieved by equilibrating a random

$\text{Si}_{0.5}\text{Ge}_{0.5}$  alloy at 300 K using a 4096-atom cubic supercell. All atoms are fourfold coordinated, and the average cohesive energy was found to be  $-4.19$  eV/atom. In Fig. 3, we plot the probability distributions  $P(E)$  of atom energies. For each type of atom (Si or Ge), we observe five distinct and narrow peaks. By inspecting the environment of atoms whose atomic energies are close to these peak values, we conclude that each peak corresponds to a different chemical environment. For Si, the first peak is at  $-4.59$  eV and corresponds to Si atoms neighboring with four Si atoms; this number coincides with the calculated cohesive energy of Si at 300 K. The second peak, at  $-4.44$  eV, corresponds to Si atoms neighboring with three Si atoms and one Ge atom. The third peak, at  $-4.29$  eV, corresponds to Si atoms neighboring with two Si atoms and two Ge atom. The last two peaks correspond to Si atoms neighboring three Ge atoms (energy  $-4.14$  eV) and Si atoms neighboring with four Ge atoms (energy  $-4.00$  eV). The five peaks in the distribution of atom energies for Ge atoms can be attributed to the same bonding environments. The peak energies and the corresponding composition of the neighbors are:  $-4.39$  eV for four Si neighbors,  $-4.25$  eV for three Si and one Ge neighbor,  $-4.11$  eV for two Si and two Ge neighbors,  $-3.95$  eV for three Si and one Ge neighbor and  $-3.81$  eV for four Ge neighbors. The last number coincides with the calculated cohesive energy of Ge at 300 K. This analysis yields values of the function  $E(c, c')$  for  $c=0$  or  $1$  and  $c' = 0.00, 0.25, 0.50, 0.75$  and  $1.00$ ; we use linear interpolation to calculate values of  $E(c, c')$  for all other values of  $c$  and  $c'$ .

We can now evaluate  $E_{el}(R)$  and  $E_{seg}(R)$  as a function of  $R$ . The strain field contributing to the elastic energy term,  $E_{el}(R)$ , will involve the superposition of the strain fields from the dislocation and the compositional segregation evident in Fig. 2. This compositional segregation, consisting of spatially separated regions of compression and tension, is clearly associated with a strain field of a dipole-like character. It will consequently fall off relatively quickly compared with the long-range dislocation strain field. With this in mind, it is appropriate to define several spatial regimes associated with the segregated dislocation: The first regime is associated with the dislocation core radius,  $R_c$ , where continuum elasticity breaks down. For segregated systems an extended core region, also exists, where significant segregation is observed. A third intermediate regime corresponds to a superposition of the compositional dipole and dislocation strains. Finally, the far-field region is dominated by the strain field for the dislocation alone. With the intention of bringing together continuum and atomistic descriptions we therefore propose a parameterization of the form

$$E_{el}(R) = b^2 k \ln(R/R_c) + E_c, \quad (4)$$

where  $R_c$  and  $E_c$  are the respective core radius and energy associated with a dislocation of Burgers vector  $\mathbf{b}$ ,

and  $k$  should depend on the region of study. In the case of an ideal continuum model of an elemental crystal, compound or ordered alloy, the factor  $k$  is formally related to elastic constants of the crystal and geometry of the dislocation [2]. In the case of segregated systems,  $k$  is expected to assume the random alloy value in the far-field region. In the intermediate and extended core regimes, the dipole segregated region around the dislocation will modify the energetics and  $k$  must be considered as an effective parameter which must be determined from atomistic calculations. Since the size of our simulation cell seems to be limited to the intermediate regime, the values of  $k$  we calculate should be smaller than the value of  $k$  for the non-segregated alloy.

In Fig. 4 we plot  $E_{el}(R)$ , as calculated using Eq. (2) as a function of  $\ln R$  in the intermediate regime. We find that the thus defined  $E_{el}(R)$  is indeed a smooth, linear function of  $\ln R$ , consistent with the parameterization scheme of Eq. (4) which effectively takes into account the influence of the extended core. We can then determine the core radius as the distance at which the linearity of  $E_{el}(R)$  breaks down. In Fig. 4, for example, this occurs at  $\ln(R/\text{\AA})=1.5$ . The core energy is then defined as  $E_c = E_{el}(R_c)$ , while  $k$  is determined by the slope of the linear region, in accordance with Eq. (4). The error in the somewhat subjective determination of  $\ln(R_c/\text{\AA})$  is about 0.05, giving an error bar of 0.05 eV/\AA for  $E_c$ . By taking the average over many runs, we determine dislocation core parameters for the alloy to be  $k = 4.5$  GPa,  $R_c = 4.5$  \AA and  $E_c = E_{el}(R_c) = 0.59$  eV/\AA. As the core parameters describe local deformations around the dislocation line, they are not very sensitive to a macroscopic strain field: For the (100)-constrained alloy, we find a marginally lower core energy (0.57 eV/\AA) and core radius (4.2 \AA). Temperature also seems to play a minor role in the core energies: at 900 K, the core energy is only 0.03 eV/\AA higher than that at 300 K.

We have evaluated the radial dependence of  $E_{seg}(R)$  directly from Eq. (3) and find a relatively weak dependence on  $R$  which can be understood from Figs. 2 and 3. Terms in Eq. (3) will be of opposite sign depending on whether  $E(c_i, c'_i)$  is associated with Ge-rich or Si-rich regions. Consequently, they will tend to cancel in the summation over a cylindrical region about the dislocation line, reflecting the symmetry of the segregated regions (Fig. 2). Therefore, we find that  $E_{seg}(R)$  can be approximated by a constant value of the order 0.2 eV/\AA. Adding this value to Eq. (4) shows that the dislocation formation energy in segregated alloys can be approximated by the continuum energy expression for a dislocation in an elemental crystal with a judicious choice of parameters appropriate to specific spatial regimes of the segregated dislocation. This surprising result indicates that simple continuum concepts, including core energies and radii, are still of value in situations where alloy segregation is significant and that the effects of the compositional

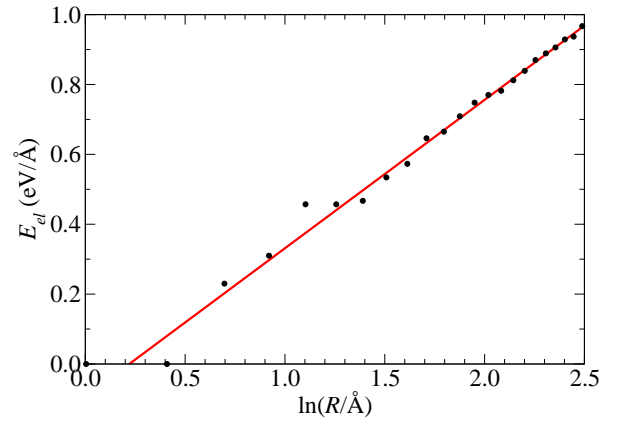


FIG. 4: (color online) Elastic energy,  $E(R)$ , contained in a cylinder of radius  $R$  and unit length around the dislocation core versus the logarithm of  $R$  for a  $60^\circ$  glide dislocation in a  $\text{Si}_{0.5}\text{Ge}_{0.5}$  alloy at 300 K.

dipole strain can be included specifically in  $k$ .

We now apply the above framework for determining core parameters in segregated systems to provide additional insight into segregation energetics by direct comparison with dislocations in idealized random alloys. This is achieved by performing simulations for dislocations in  $\text{Si}_{0.5}\text{Ge}_{0.5}$  alloys artificially constrained to have a random occupation of the lattice sites. We find that the dislocation formation energy (3.7 eV/\AA) is 2.0 eV/\AA greater than in the segregated alloy (1.7 eV/\AA). Surprisingly, however, the ideal random alloy has a smaller core radius of 3.9 \AA with a correspondingly lower core energy of 0.31 eV/\AA, as determined by a linear fit of Eq. (4). The parameter  $k$  of Eq. (4) is found to be 5.4 GPa. This value is, larger than the value found for the segregated alloy, as expected.

To understand this we note that preventing atoms to exchange identities and occupy their energetically favored sites around the dislocation core results in weaker bonds in this area which are easier to deform. This explains the lower core energies associated with perfectly random alloy systems. However, despite higher core energies, the significant segregation outside of the core radius  $R_c$  (Fig. 2) lowers the overall dislocation formation energy for segregated systems by reducing the overall elastic energy  $E_{el}(R)$ .

In summary, by partitioning the dislocation formation energy into elastic and segregation components we have established a general framework for calculating the core properties of dislocations in segregated alloys. This approach opens up new possibilities for the study of more complex processes such as ‘alloy drag’ on the motion of dislocations [15], the influence of local segregation (including vacancies) on the Peierls barrier and kink mobility [16], as well as dislocation-induced segregation in confined systems such as quantum dots.

I. R. acknowledges useful discussions with Dr. J. Schiotz. We are particularly grateful to an anonymous referee for providing valuable insight into the continuum description of segregated dislocations. This work is supported by a grant from the EU and the Ministry of National Education and Religious Affairs of Greece through the action “ΕΠΕΑΕΚ” (programme “ΠΥΘΑΓΟΡΑΣ.”) D. E. J. is funded by the ARC.

---

<sup>†</sup> Electronic address: [remed@physics.uoc.gr](mailto:remed@physics.uoc.gr)

- [1] R. Hull, J. C. Bean, and C. Buescher, *J. Appl. Phys.* **66**, 5837 (1989).
- [2] J. P. Hirth and J. Lothe, *Theory of Dislocations* (McGraw Hill, 1968).
- [3] T. A. Arias and J. D. Joannopoulos, *Phys. Rev. Lett.* **73**, 680 (1994).
- [4] X. Blase *et al.*, *Phys. Rev. Lett.* **84**, 5780 (2000).
- [5] A. T. Blumenau *et al.*, *Phys. Rev. B* **65**, 205205 (2002); A. T. Blumenau *et al.*, *J. Phys: Cond. Matt.* **14**, 12741 (2002).
- [6] L. Martinelli *et al.*, *Appl. Phys. Lett.* **84**, 2895 (2004).
- [7] See, for example, D. C. Houghton *et al.*, *J. Appl. Phys.* **67** 1850 (1990).
- [8] I. A. Ovid'ko, *Phys. Rev. Lett.* **88**, 046103 (2002).
- [9] U. Denker and D. E. Jesson, *Phys. Stat. Sol. (b)* **242**, 2455 (2005).
- [10] J. Tersoff, *Phys. Rev. B* **39**, 5566 (1989).
- [11] P. C. Kelires and J. Tersoff, *Phys. Rev. Lett.* **63**, 1164 (1989).
- [12] P. C. Kelires, *Phys. Rev. Lett.* **75**, 1114 (1995); *Surf. Sci.* **418**, L62 (1998).
- [13] A. Marzegalli, F. Montalenti, and L. Miglio, *Appl. Phys. Lett.* **86**, 041912 (2005).
- [14] The dislocation strain field is introduced by employing the Atomic Simulation Environment, ASE; see <http://www.camp.dtu.dk/Software>.
- [15] Y. Wang *et al.*, *Acta mater.* **48**, 2163 (2000).
- [16] J. K. Ternes, D. Farkas and R. Kriz, *Phil. Mag. A* **72**, 1671 (1995); D. Farkas *et al.*, *Acta Materialia* **44**, 409 (1996).